Nup2p Dynamically Associates with the Distal Regions of the Yeast Nuclear Pore Complex

David J. Dilworth,*‡ Adisetyantari Suprapto,§ Julio C. Padovan,§ Brian T. Chait,§ Richard W. Wozniak,‡ Michael P. Rout,‡ and John D. Aitchison*‡

*Institute for Systems Biology, Seattle, Washington, 98105; ‡Department of Cell Biology, University of Alberta, Edmonton, Canada, T6G 2H7; and §The Rockefeller University, New York, New York, 10021

Abstract. Nucleocytoplasmic transport is mediated by the interplay between soluble transport factors and nucleoporins resident within the nuclear pore complex (NPC). Understanding this process demands knowledge of components of both the soluble and stationary phases and the interface between them. Here, we provide evidence that Nup2p, previously considered to be a typical yeast nucleoporin that binds import- and export-bound karyopherins, dynamically associates with the NPC in a Ran-facilitated manner. When bound to the NPC, Nup2p associates with regions corresponding to the nuclear basket and cytoplasmic fibrils. On the nucleoplasmic face, where the Ran–GTP levels are predicted to be high, Nup2p binds to Nup60p. Deletion of *NUP60* renders Nup2p nucleoplasmic and compromises Nup2p-mediated recycling of Kap60p/Srp1p. Depletion of Ran–GTP by metabolic poisoning, disruption of the Ran cycle, or in vitro by cell lysis, results in a shift of Nup2p from the nucleoplasm to the cytoplasmic face of the NPC. This mobility of Nup2p was also detected using heterokaryons where, unlike nucleoporins, Nup2p was observed to move from one nucleus to the other. Together, our data support a model in which Nup2p movement facilitates the transition between the import and export phases of nucleocytoplasmic transport.

Key words: nucleoporin • nuclear transport • karyopherin • importin • exportin

Introduction

The structure of the nuclear pore complex (NPC)[1] is highly conserved among eukaryotes, having eightfold symmetry in the plane perpendicular to the nuclear envelope (NE) and twofold pseudo-symmetry in the plane parallel to the NE (for reviews see Allen et al., 2000; Wente, 2000; Rout and Aitchison, 2001). The NPC consists of a central tube, termed the central transporter, anchored in the NE by a spoke ring structure. Cytoplasmic fibrils extend into the cytoplasm, and nuclear fibrils connect at the distal end to form the nuclear basket. In the budding yeast, *Saccharomyces cerevisiae*, the NPC consists of ~30 protein subunits termed nucleoporins. Each nucleoporin is present in multiple copies per NPC, which accounts for the large molecular mass of this structure (~50 MD in yeast) (Rout et al., 2000). Nucleoporins can be subdivided into two groups: those that contain phenyalanine–glycine repeats (FG-nups) and those that do not. The repeat domains are important binding sites for transport factors as they traverse the NPC (Bayliss et al., 2000). Immunoelectron microscopical localization of protein A (pA)–tagged nucleoporin chimeras reveals that the majority of nucleoporins, including FG-nups, are present within the core region of the NPC and are symmetrically distributed on the nuclear and cytoplasmic faces. In addition, a small number of nups appear to be biased to one side of the NPC but are present on both faces. Nup1p and Nup60p, both FG-nups, localize solely to the distal nucleoplasmic face of the NPC and likely form the nuclear basket. Similarly, three nups are found only on the cytoplasmic face: the FG-nups, Nup159p and Nup42p, and the non–FG-nup, Nup82p. These nups likely constitute the cytoplasmic fibrils (Stoffler et al., 1999; Rout et al., 2000).

Numerous soluble transport factors act in concert to mediate translocation across the NPC and provide energy to transport. Members of the karyopherin (kap) family (karyopherin/importins/exportins) recognize specific subsets of cargoes through either a nuclear localization signal (NLS), for import substrates, or a nuclear export signal (NES) for export substrates. There are 14 kap family

Address correspondence to John Aitchison, Institute for Systems Biology, 4225 Roosevelt Way, Suite 200, Seattle, WA 98105-6099. Tel.: (206) 732-1344. Fax: (206) 732-1299. E-mail: jaitchison@systemsbiology.org

[1]*Abbreviations used in this paper:* cNLS, classical NLS; FG-nup, phenylalanine–glycine repeat nucleoporin; GFP, green fluorescent protein; GST, glutathione *S*-transferase; IEM, immunoelectron microscopy; kap, karyopherin; NE, nuclear envelope; NES, nuclear export signal; NLS, nuclear localization signal; NPC, nuclear pore complex; pA, protein A; RBD, Ran binding domain.

members in yeast (for review, see Mattaj and Englmeier, 1998; Pemberton et al., 1998; Wozniak et al., 1998). Each kap has the ability to interact with numerous FG-nups (for review see Ryan and Wente, 2000), suggesting that translocation is mediated by a series of binding and release steps spanning the length of the NPC (Blobel, 1995; Rexach and Blobel, 1995). In addition, although making several interactions, kaps bind to a discreet subset of FG-nups, such that they likely traverse the NPC by overlapping, but distinct routes (Aitchison et al., 1996; Rout et al., 1997; Marelli et al., 1998; Damelin and Silver, 2000).

Although most kaps bind to both their cargoes and components of the NPC directly (Pemberton et al., 1998; Wozniak et al., 1998), the first nuclear transport pathway to be characterized proved to be an exception to this generality. In this case, proteins harboring a classical NLS (cNLS) are recognized by the Kap α/β heterodimer (Kap60p/Srp1p and Kap95p, respectively, in yeast). The Kap60p subunit acts as an adaptor for Kap95p, binding to cNLS and forming a stable trimeric import complex (Rexach and Blobel, 1995; Weis et al., 1995; Conti et al., 1998). Kap95p in turn interacts with FG-nups (Rexach and Blobel, 1995, Aitchison et al., 1996), facilitating movement of the complex across the NPC to the nuclear basket where the complex dissociates and the cargo is released into the nucleus (Gorlich et al., 1996).

Cargo release is mediated by the small GTPase Ran (Rexach and Blobel, 1995; for reviews see Cole and Hammell, 1998; Moore, 1998). Ran primarily exists in two forms in the cell: bound to either GDP or GTP. Although it has not been directly measured, it is believed that the nuclear pool of Ran is primarily GTP-bound, maintained by the nuclear-restricted Ran guanylyl–nucleotide exchange factor (RanGEF/RCC1; Prp20p/Srm1p/Mtr1p in yeast). In contrast, the cytoplasmic pool of Ran is maintained in its GDP-bound form by the presence of the cytoplasmic Ran GTPase-activating protein (RanGAP; Rna1p in yeast). The interaction between an import-bound kap and an NLS is stable in the cytoplasmic environment of Ran-GDP, but in the nucleus, Ran-GTP binds to the kap, causing it to release its cargo (Rexach and Blobel, 1995). The opposite is true of export-bound kaps. In this case, the interaction of Ran-GTP with the kap promotes the cooperative binding of the NES (Fornerod et al., 1997), but upon transport to the cytoplasm, the GTP is hydrolyzed and the cargo is released (for review, see Görlich and Kutay, 1999). It has also been demonstrated that Ran-GTP stimulates the release of import-bound kaps from specific nucleoporins (Rexach and Blobel, 1995; Gorlich et al., 1996), whereas export-bound kaps interact with nucleoporins in the presence of Ran-GTP (Kehlenbach et al., 1999). Thus, this proposed steep gradient of Ran-GTP versus Ran-GDP across the NE is central to our current view of nuclear transport. However, the mechanism of selective and directional movement of kap/cargo complexes through the NPC is yet to be determined.

To fully understand this process, it is necessary to identify all the components of the transport machinery and characterize how constituents of the NPC interact with mobile factors that cycle on and off the NPC to mediate cargo movement. Recently, a comprehensive analysis of the yeast NPC led to the proposal that the NPC functions as a Brownian affinity gate (Rout et al., 2000). In this model, the narrow central transporter and the Brownian motion of the surrounding filamentous FG-nups restrict macromolecular passage through the NPC. Cargo-carrying transport factors that have an affinity for the FG-nups use their binding energies to overcome this entropic exclusion. Directional transport through the NPC is accomplished by contributions from both the few FG-nups localized to the nuclear or cytoplasmic face of the NPC and the asymmetric distribution of GTP- and GDP-Ran.

One of the major goals of that comprehensive study was to establish testable models of NPC function by compiling the inventory of yeast nucleoporins. In so doing, bona fide nucleoporins were classified as such if they showed in vivo localization with known NPC markers and coenriched with NPCs in biochemical subcellular fractionation experiments. During this analysis, Nup2p, previously characterized as a yeast nucleoporin (Loeb et al., 1993), failed to meet all of these criteria, and was therefore not classified as a nucleoporin. Here, we reexamine this classification and establish that Nup2p lies at the boundary between the NPC and the mobile phase of transport, moving on and off the NPC in a Ran-dependent manner and mediating interactions typical of both transport factors and nucleoporins.

Materials and Methods

Strains and Plasmids

Haploid strains expressing chromosomal fusions of the gene encoding *Staphylococcus aureus* pA to *NUP2*, *NUP159*, *KAP95*, *NUP1*, and *NUP60* were obtained in DF5 cells as previously described (Aitchison et al., 1995b, 1996; Rout et al., 2000). A Nup60p–pA strain lacking Nup2p was created by crossing the Nup60p–pA strain (Nup60p–pA[*HIS5*]) to a Δ*nup2* strain, LDY627 (*nup2::TRP1*; Booth et al., 1999), and subsequent isolation of Nup60p–pA Δ*nup2* spores. Similarly, a Δ*nup60* strain, JAY1331, created by deletion/disruption with a *TRP1* cassette, was used to generate a Nup2p–pA strain lacking Nup60p. Chromosomal green fluorescent protein (GFP) fusions to *NUP2*, *NUP49*, *NSP1*, *NUP159*, *NUP60*, *CSE1*, *KAP60*, and *KAP95* were created in an identical manner to the pA–tagged strains, except that the region encoding *S. aureus* pA downstream of amino acid 54 was replaced with the gene encoding *Aequoria victoria* GFP (Stade et al., 1997) to generate the pGFP/HIS5 tagging vector. A Nup2p–GFP mutant lacking the Ran binding domain (RBD) was created using the same technique, except oligonucleotides were designed to eliminate amino acids 606–720 of Nup2p upon integration of the GFP tag to generate Nup2ΔRBD–GFP. To allow GFP tagging where the oligonucleotides were originally designed for the pProtA/HU tagging vector (Aitchison et al., 1995b), we ligated a short sequence containing the pProtA/HU reverse oligonucelotide annealing site into pGFP(HIS5) downstream of the *HIS5* marker.

The Nup2p–GFP strain was crossed to a strain lacking Nup120p (*nup120::URA3*) (Aitchison et al., 1995a), and cells were sporulated to generate Nup2p–GFP Δ*nup120* haploid cells. To create a Nup2p–GFP Δ*nup1* strain, the Nup2p–GFP strain was crossed to a *NUP1* null strain, KBY51 (*nup1-2::LEU2*) (Belanger et al., 1994), containing the pLDB73 covering plasmid (*CEN URA3 ADE3 NUP1*), sporulated, and appropriate haploid strains were grown on 5-fluoroorotic acid to eliminate the covering plasmid. JAY1331 was used to generate Nup2p–GFP, Nup49p–GFP, and Nsp1p–GFP strains in a Δ*nup60* background. A galactose-inducible *NUP60* plasmid was generated by PCR amplification of *NUP60* from *S. cerevisiae* genomic DNA using primers containing flanking *BamH1* restriction sites. This PCR product was cloned into the *BamH1* site of pYES2 (CLONTECH Laboratories, Inc.). Strains Kap60p–GFP Δ*nup2*, Kap60p–GFP Δ*nup60*, and Kap60p–GFP Δ*nup100* were created by crossing strains LDY627, JAY1331, and SWY1017 (*nup100::HIS3*) (Murphy et al., 1996) to JBY1 (*SRP1–GFP[LEU2]*) (Booth et al., 1999).

Strains used to analyze genetic interactions between *NUP2* and *NUP60* were derived by crossing JAY1331 to LDY680 (*nup2::KAN^R*) (Booth et al., 1999) with covering plasmids pLDB60 (encoding full-length Nup2p) or

pLDB690 (Nup2p amino acids 1–546; Booth et al., 1999) and isolation of wild-type, single, and double mutant spores. Genetic interactions between *NUP60* and *KAP60* were analyzed by crossing JAY1331 cells to strain NOY612, which harbors the *srp1-31* temperature-sensitive mutation (Yano et al., 1994), and isolation of relevant spores.

The *prp20-7* temperature-sensitive allele was introduced into GFP-tagged strains by crossing Nup2p–GFP, Nup2p–GFP Δ*nup60*, Nup49p–GFP, and Kap60p–GFP strains to $M_3$16/1A (*prp20-7*; Amberg et al., 1993) and isolating of relevant spores. Heterokaryon shuttling assays were performed using a *kar1-1* karyogamy mutant strain, MS739 (Vallen et al., 1992; Bucci and Wente, 1997).

Microscopy

Immunoelectron microscopy (IEM) localization of pA–tagged nups was carried out as described (Kraemer et al., 1995; Nehrbass et al., 1996; Rout et al., 2000) for NEs and as described (Strambio-de-Castillia et al., 1999) for intact nuclei. GFP fluorescence was visualized by confocal microscopy using a confocal microscope (LSM 510 NLO; Carl Zeiss, Inc.).

Heterokaryon Shuttling Assay

Equal volumes of midlog phase *kar1-1* (*MAT*α) cells and genomically integrated GFP-tagged strains (*MATa*) grown in selective media with 2% glucose at 23°C were mixed and pelleted by brief centrifugation. The cell pellet was resuspended in 200 μl of complete synthetic media (CSM) with 2% glucose and incubated for 30 min at room temperature without agitation. Samples were then mixed gently and prepared for confocal microscopy by placing 50 μl on a microscope slide coated with 200 μl of 2% agarose glucose–CSM. Coverslips were placed over the samples and sealed to prevent drying. Slides were incubated at room temperature for an additional 3 h to allow mating followed by simultaneous acquisition of GFP fluorescence and bright field signals for 30 min. Mating cells were scored as shuttling if GFP signal was detected in two well-separated nuclei, as nonshuttling if GFP signal was only detected in one nuclei, or as inconclusive when the nuclei displaying GFP fluorescence were not clearly separated and thus could be confused with the onset of nuclear fission. For time course shuttling experiments, z-stacks of ~5-μm slices were acquired at 20-min intervals (usually 10 slices per time point stack). Analysis was performed on a Macintosh G4 Cube computer using the public domain NIH Image program v1.62 (developed at the U.S. National Institutes of Health) essentially as described by Bucci and Wente (1997), with the exception that nonmating Nup–GFP cells were also quantitated to measure the bleaching due to sample acquisition.

Quantitation of Nucleoporin Expression Levels by Analytical Flow Cytometry

Logarithmically growing liquid cultures of Nup–GFP (*MATa*) strains as well as an untagged DF5 (*MATa*) strain were analyzed using a Becton Dickenson FACSCalibur® flow cytometer and CELLQuest software. A total of 10,000 events were measured for each acquisition, and cells were gated based on the SSC and FSC to limit the analysis to cells of uniform size and granularity. After gating, between 5,000 and 8,000 events remained for analysis and the mean GFP fluorescence (FL1) was calculated for each sample. Each acquisition was repeated in triplicate to ensure run-to-run consistency. Error in these repeated measurements was never >2%. The mean GFP intensity was normalized by subtraction of the mean intensity of the DF5 control (representing background autofluorescence). Four independent experiments were performed, and the average normalized fluorescence and standard deviation of the experiments were calculated for each protein.

Photobleach/Recovery Turnover Assay

Nup2p–GFP (*MATa*) and Nup49p–GFP (*MATa*) cells were grown to midlog phase at 23°C in selective media containing 2% glucose. Slides were prepared as described above. Cells in a single field of view were photobleached with 30 iterations of the 488-nm wavelength at 40% power in an area encompassing only the nucleus or the entire cell. Z-stacks (typically 10 slices of 0.5 μm each) were acquired before bleaching, directly after bleaching, and 20, 40, and 60 min after bleaching. Data were analyzed with NIH Image as for heterokaryon experiments, with the exception that the mean fluorescence of bleached cells was normalized for sample acquisition bleaching by the rate of signal loss in unbleached controls over the course of the experiment.

Whole Cell Lysate Immunoprecipitations

pA–tagged strains were grown to late log phase (~5×10^7 cells/ml). Cells from two-liter cultures were harvested, washed, and resuspended in lysis buffer (20 mM Na_2HPO_4, pH 7.5, 150 mM NaCl, 0.1 mM $MgCl_2$, 2 μg/ml pepstatin A, and 90 μg/ml PMSF). The resuspended cells were passed through a French pressure cell and then diluted twofold by the addition of lysis buffer containing 40% DMSO and 2% Triton X-100. Cellular debris were pelleted by centrifugation at 15,000 rpm for 15 min in a Beckman Coulter JA25.50 rotor. The supernatant from this low-speed spin was further clarified by centrifugation at 45,000 rpm for 90 min in a Beckman Coulter type70 Ti rotor. This soluble protein fraction was then incubated on a rocker overnight at 4°C with 50 μl of preequilibrated IgG–Sepharose (Amersham Pharmacia Biotech.). IgG–Sepharose was harvested by centrifugation and washed three times with 1 ml wash buffer (20 mM Na_2HPO_4, pH 7.5, 150 mM NaCl, 0.1 mM $MgCl_2$, 0.1% Tween 20, 2 μg/ml pepstatin A, and 90 μg/ml PMSF) followed by three additional washes in wash buffer containing 50 mM $MgCl_2$. Bound proteins were eluted in wash buffer containing increasing concentrations of magnesium chloride (0.1, 0.2, 0.5, 1.0, 2.0, and 4.0 M), concentrated by TCA precipitation and resolved by SDS-PAGE. Coimmunopurifying proteins were identified by SDS-PAGE and mass spectrometry as described (Rout et al., 2000).

Immunoblotting

Eluted proteins from Nup60p–pA immunopurifications of wild type and cells lacking Nup2p were resolved by SDS-PAGE, immobilized on nitrocellulose membranes, and immunoblotted by standard procedures. Immunoreactive bands were detected with the Super Signal ECL system (Pierce Chemical Co.) using a Fluorchem 8000 digital imager (Alpha Innotech Corporation). Anti-Srp1p antibodies were a gift of Laura Davis (Booth et al., 1999). Rabbit polyclonal Nup2p antibodies were raised against recombinant purified glutathione *S*-transferase (GST)-Nup2p and affinity depleted of anti-GST antibodies by incubation with recombinant purified GST bound to glutathione–Sepharose beads.

Galactose Induction of Nup60p

The pGAL-NUP60 plasmid was transformed into Nup2p–GFP cells lacking Nup60p, and these cells were grown to midlog phase at 23°C in selective media containing 2% glucose. Initial images of uninduced cells were acquired at this time after which cells were spun down, resuspended in selective media containing 2% galactose, grown for 5 h at 23°C, and visualized again.

Quantitation of Fluorescent Intensity along Nuclear Bisects

To determine the relative amount of intranuclear signal in Nup2ΔRBD–GFP compared with Nup2p–GFP in wild-type and Δ*nup60* backgrounds, cells from single confocal slices were analyzed using the Plot Profile tool in NIH Image. Lines (4 pixels wide) were drawn to bisect the nucleus; thus, the profiles obtained are the average fluorescent intensity of four adjacent pixels across the length of the nucleus. Profiles were oriented with the nucleolus to the left in cases where the nucleolus was detectable, due to the exclusion of GFP signal from this organelle. The numerical data was exported to Microsoft Excel, and montages for 15 cells were compiled. The average and standard deviation of the data were also determined as an indication of the variability of the nuclear fluorescence.

Metabolic Poisoning

Cells were grown to midlog phase at 23°C in selective media containing 2% glucose and were visualized. After initial image acquisition, cells were centrifuged, washed once with sterile water, resuspended in sterile water containing 10 mM deoxyglucose and 10 mM sodium azide, and incubated at room temperature without agitation (Shulga et al., 1996). GFP signal was monitored at 15-min intervals for 45 min. Cells were then spun down and recovered in selective media containing 2% glucose for 10 min and visualized again.

prp20-7 Temperature Shift

Strains were grown to midlog phase at 23°C in 2 ml CSM containing 2% glucose. Slides were prepared for confocal microscopy as described under above. Zero time point images were acquired, after which slides were in-

cubated at 37°C for 90 min, and observed. After the temperature shift, cells were recovered at 23°C for 1 h and visualized again.

Results

The Localization of Nup2p at the NPC

Nup2p has several characteristics consistent with its initial classification as a nucleoporin: it contains repeat motifs of FG-nups and gives a punctate NE fluorescence microscopy pattern typical of nucleoporins. However, two pieces of evidence suggest that Nup2p is not a typical yeast nucleoporin. First, immunopurification of Kap95p–pA from yeast cytosol (under conditions where no other known nucleoporins are liberated) yields significant amounts of Nup2p (Aitchison et al., 1996; Rout et al., 1997). Second, unlike nucleoporins, Nup2p does not coenrich with either NPCs (Rout and Blobel, 1993) or NEs; rather, a substantial portion of Nup2p is found in both the nucleoplasmic and cytoplasmic fractions. Indeed, the subcellular fractionation profile of Nup2p is more similar to the profiles obtained for transport factors, such as Kap120p, Kap122/Pdr6p (Rout et al., 2000), Kap95p, and Kap123p (Rout et al., 1997). Both lines of evidence argue for a weak, perhaps transient, interaction between Nup2p and the NPC. Because of this anomalous behavior, we sought to localize Nup2p with greater precision, monitor its distribution under different conditions, and characterize its interaction with the NPC using fully functional genomically encoded fusions of the genes encoding *Staphylococcus aureus* pA or *Aequoria victoria* GFP appended to the 3′ end of the *NUP2* coding region (Aitchison et al., 1995b; Rout et al., 2000).

We hypothesized that, since only a portion of Nup2p copurified with NEs, there may be different pools of Nup2p that might be found at different locations in intact nuclei, compared with purified NEs. To this end, Nup2p–pA was localized in both nuclei and NE subcellular fractions by preembedding labeling and IEM (Kraemer et al., 1995; Nehrbass et al., 1996). In NEs, Nup2p–pA was present solely at the distal nuclear face of the NPC (Fig. 1 A), significantly further from the midplane of the NPC than control nups (Rout et al., 2000). However, when the same procedure was used on isolated nuclei, Nup2p–pA was found on both the nuclear and cytoplasmic sides of the NPC (Fig. 1 B). Because the isolation of nuclei precedes the subsequent partial solubilization of Nup2p from the NE fraction, we have potentially revealed a separate specific location for that fraction of Nup2p liberated upon the isolation of NEs. These data suggest that there are at least two distinct sites, on either side of the NPC, to which Nup2p can bind. As controls, we also determined the positions of Nup159p–pA and Nup1p–pA. The relative positions of these two nucleoporins with respect to each other and the nuclear portion of Nup2p–pA were similar in both purified NEs and intact nuclei (summarized in Fig. 1 C). This suggests that the dual localization of Nup2p is not due to gross alteration of NPC morphology between preparations. Notably, the signal for each nup is further from the NE midplane when visualized on isolated NEs than on correspondingly labeled isolated nuclei. This is likely caused by hypotonic shock and the removal of constraining chromatin during NE isolation, resulting in a measured ~40% increase in the thickness of the NE and hence, its associated structures (data not shown). However, as the relative positions between nups remain similar (Fig. 1; Rout et al., 2000), the conclusions of these localizations remain unaffected. Such preparation-dependent changes have been widely acknowledged (King and Baskin, 1991; Smitherman et al., 2000), even for the NPC (Akey, 1995), and sound a note of caution when attempting to directly compare data derived from different preparation techniques.

The presence of Nup2p on both sides of the NPC in nuclei suggests that during the solubilization and purification of NEs, Nup2p is preferentially retained at the nuclear face. This may be explained if Nup2p is a resident of the NPC and, like most nucleoporins, symmetrically localized to both sides of the NE, but the relatively weak interaction of Nup2p with components on the cytoplasmic face is disrupted during the preparation of NEs. On the other hand, whole cell IEM procedures reveal the majority of Nup2p signal at the nucleoplasmic face of the NPC (Hood et al., 2000; Solsbacher et al., 2000). To explain this apparent discrepancy, as well as the presence of Nup2p in the soluble phase of transport, we hypothesized that Nup2p may be in constant movement between these two NPC binding sites and the conditions used during the preparation of nuclei promotes its movement to the soluble pool and the cytoplasmic face. To test this hypothesis, and identify factors that promote this mobility, we first investigated if we could detect the movement of Nup2p in vivo.

Nup2p Is Mobile

To test for Nup2p mobility, we created yeast heterokaryons and assayed for movement of Nup2p between two adjacent nuclei. In this assay, a strain containing a genomically integrated gene fusion encoding a GFP-tagged nucleoporin (donor) was mated with a *kar1-1* strain (recipient), which is defective in nuclear fusion after mating (Vallen et al., 1992). Thus, mated cells fuse, sharing a common cytoplasm, but their nuclei remain separate. We predicted that under these conditions, a nucleoporin stably associated with the NPC would remain in the donor NPC, whereas a protein that continuously cycles between NPC docking sites would enter the soluble phase and quickly appear at the NPC of the recipient nucleus. We monitored the GFP signal in fused cells containing Nup2p–GFP and the control nucleoporins Nup49p–GFP (Fig. 2 A), Nup60p–GFP, and Nsp1p–GFP (data not shown). Each control nucleoporin remained entirely in the donor NPC during the course of the assay, but Nup2p–GFP signal was not restricted to the original nucleus and appeared in the *kar1-1* recipient nucleus. Under the conditions used here, cell fusion was first detected ~3 h 15 min after the initial mixing of the strains. Nup2p–GFP was first detectable in some *kar1-1* nuclei within the next 15 min with an increasing number of mated cells exhibiting fluorescence signal over a subsequent 30-min time period. The number of detectably fluorescent recipient nuclei is presented in Fig. 2 B. Only clearly separated nuclei were scored as positive. Heterokaryons in which it was difficult to distinguish separate nuclei, as opposed to dividing nuclei, were scored as inconclusive. Nup2p was the only nucleoporin assayed that exhibited movement from the donor to the recipient NPC in this time

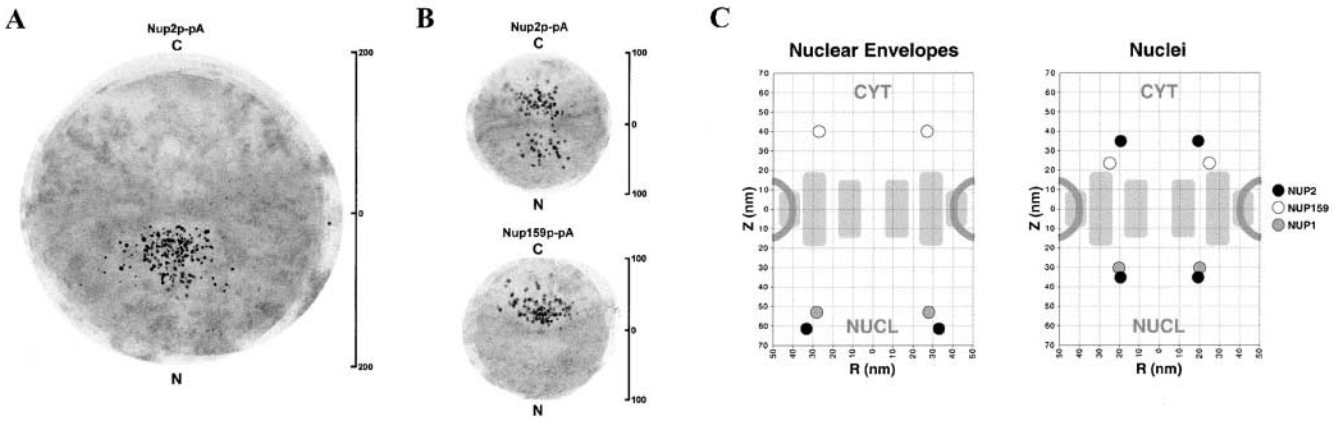

Figure 1. Nup2p localizes to multiple sites within the NPC. Nup2p–pA was localized in purified NEs (A) and nuclei (B) by IEM using gold-conjugated antibodies. Montages of 20 NPCs were prepared with the cytoplasmic side of the NPCs oriented up (determined by the presence of ribosomes on the NE). In NEs, Nup2p–pA localized solely to the nuclear face of the NPC ~63 nm from the midplane of the NPC. In intact nuclei, Nup2p–pA was detected on both faces of the NPC ~36 nm from the midplane. For comparison, Nup159p–pA and Nup1p–pA (not shown) were also localized under these conditions, demonstrating that the relative localization of Nup1p–pA, Nup159p–pA, and nuclear Nup2p–pA did not vary significantly between the different preparations. The positions of Nup2p–pA, Nup159p–pA, and Nup1p–pA in each montage is summarized in C.

frame. Observation of heterokaryons at later time points revealed that Nup2p–GFP equilibrates between the donor and recipient nuclei between 60 and 120 min after cytoduction, at which point there is a modest signal detectable in most Nup49p–GFP heterokaryons (data not shown). The appearance of Nup49p–GFP signal in the recipient nucleus after this time period is consistent with reports of the assembly rate of new NPCs (Bucci and Wente, 1997).

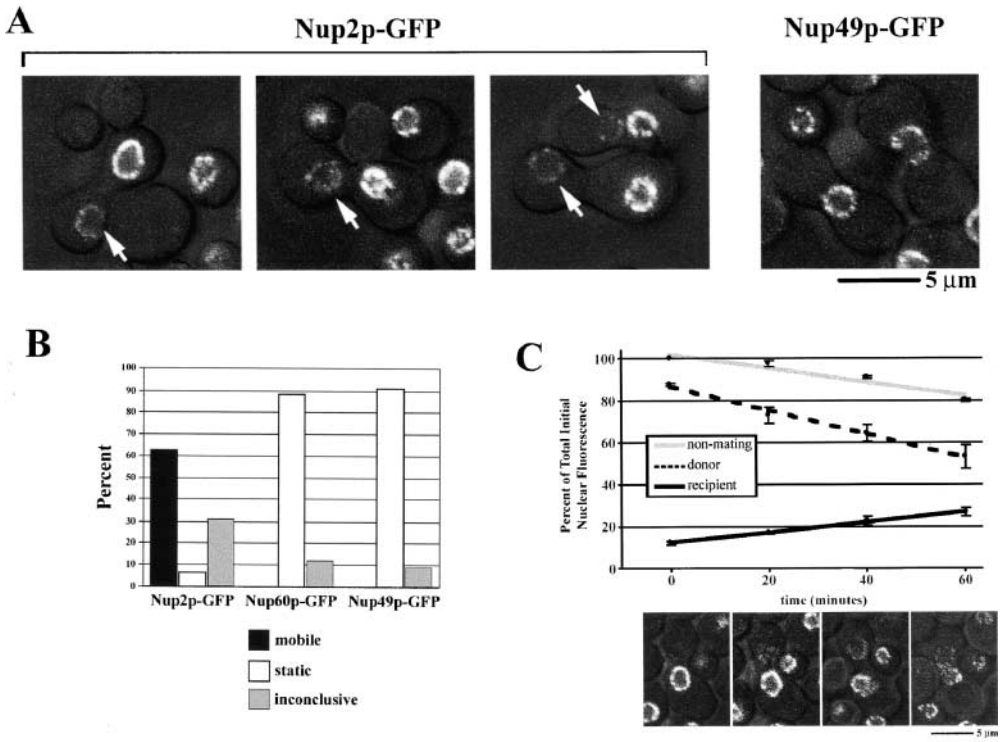

Figure 2. Nup2p is mobile. (A) Confocal images of bright field and GFP fluorescence acquired 15–45 min after heterokaryon formation. Nup2p–GFP signal is detectable in the recipient *kar1-1* nucleus during this time (Nup2p–GFP), whereas Nup49p–GFP remained in the donor nucleus (Nup49p–GFP). Other control nucleoporins, Nup60p and Nsp1p, were also detected only in the donor nucleus over these time courses (data not shown). (B) Summary of nucleoporin mobility assay results. Heterokaryons were scored as mobile if GFP signal was detected in two well-separated nuclei; static, if only one fluorescing nucleus could be seen or inconclusive in situations where it was difficult to distinguish between a dividing donor nucleus or adjacent donor/recipient nuclei. In the time interval tested, >60% of Nup2p–GFP heterokaryons exhibited GFP signal in a clearly distinct recipient nucleus, whereas we detected no movement in Nup60p–GFP and Nup49p–GFP heterokaryons over this time course. The percentage of inconclusive heterokaryons reported for Nup2p–GFP was significantly higher than that for control nucleoporins, which likely reflects the conservative nature of the classification. (C) Gain of signal in the recipient nucleus of Nup2p–GFP heterokaryons is concomitant with a loss of fluorescence in the donor nucleus. Nup2p–GFP heterokaryons were monitored for 1 h, and the percentage of the total initial nuclear fluorescence for the donor and recipient nuclei are plotted over time. Shown below are representative image slices at each time point. The fluorescence of a nonmating Nup2p–GFP cell in the same field of view was also determined to show sample acquisition bleaching. All plots are the average of two heterokaryons/cells, and error bars represent the standard deviation of the two measurements.

The appearance of Nup2p–GFP in the recipient nucleus could be due to (a) movement from one nucleus to another, which would indicate that Nup2p is indeed a mobile component of the NPC; (b) a significant cytoplasmic pool of Nup2p–GFP that goes undetected by visual observation of the fluorescence signal; or (c) a rapid turnover of Nup2p–GFP and, therefore, high synthesis and degradation rate. To distinguish among these possibilities, we first monitored the movement of Nup2p–GFP in heterokaryons and, through quantitation of the fluorescence signal in the donor and recipient nuclei, established that the appearance of fluorescent signal in the recipient nucleus is coincident with a decrease in the donor nucleus signal (Fig. 2 C). This precursor–product relationship between the fluorescent intensity of the donor and recipient nuclei suggests that Nup2p–GFP signal appearing in the recipient nucleus is derived from the donor nucleus and that Nup2p is capable of moving from one nucleus to another. We detected no movement of Nup49p–GFP from the donor to the recipient nucleus in this assay (data not shown).

To eliminate the possibility of a rapid turnover rate or a significant cytoplasmic pool of Nup2p, we first compared the relative cellular levels of Nup2p–GFP with nucleoporins using analytical flow cytometry (Fig. 3 A). In this assay, the fluorescence signal from Nup2p–GFP was approximately half of that of Nsp1p–GFP, twice that of Nup60p–GFP and Nup159p–GFP, and equivalent to the signal from Nup49p–GFP. These data fit well with our previous estimates of the abundance of nups by quantitative immunoblotting using pA-tagged nucleoporins in isolated NEs (Rout et al., 2000) and suggest that Nup2p, like Nup49p, is present at approximately two copies per octagonally symmetric NPC subunit.

Given that the abundance of Nup2p is similar to Nup49p, if the appearance of Nup2p–GFP in the recipient nucleus were due to new synthesis, Nup2p would have to be synthesized (and degraded) at significantly higher rates than Nup49p. Thus, we compared the turnover of Nup2p to that of Nup49p using a fluorescence bleach/recovery experiment in real time. In this experiment, the GFP signal was photobleached in either the nuclear compartment or over the entire cell, and the recovery of fluorescence was quantitated. Not only did this assay provide an estimation of protein turnover and maturation rates, it also allowed us to test for the existence of a significant cytoplasmic pool of Nup2p by comparing the recovery rates for cells that were entirely bleached to those where only the nucleus was bleached. If there is a significant cytoplasmic pool of Nup2p, capable of exchanging with NPC-associated Nup2p, we would predict that in cells where only the nucleus was bleached, the fluorescent signal would recover at a faster rate than in cells subjected to whole cell bleaching. As shown in Fig. 3 B, the rate of fluorescence recovery for Nup2p–GFP was equivalent to that of Nup49p–GFP, irrespective of the bleached region. Together, these data lead us to conclude that the appearance of Nup2p–GFP in the recipient *kar1-1* nucleus in the heterokaryon experiments was due to the movement of Nup2p–GFP specifically from the donor nucleus, rather than from de novo synthesis or from a cytoplasmic pool.

Nup2p Binds to Kap60p, Kap95p, and the Nucleoporin Nup60p

To further characterize the interaction of Nup2p with the NPC, Nup2p–pA was immunoisolated from whole cell lysates to identify any interacting proteins. As expected and observed previously, both Kap60p and Kap95p copurified with Nup2p–pA; however, although NPCs were disrupted under these conditions (Marelli et al., 1998) (see below), we identified no copurifying nucleoporins (Fig. 4 A). Because the IEM data presented above suggests that Nup2p binds with a relatively high affinity to the nuclear face of the NPC and this interaction is stable to the disruption of nuclei, we attempted to immunopurify Nup2p in a complex with either Nup1p–pA or Nup60p–pA. These two proteins were chosen as candidate Nup2p binding partners because they are the only nucleoporins asymmetrically localized to the distal nuclear face of the NPC (Rout et al.,

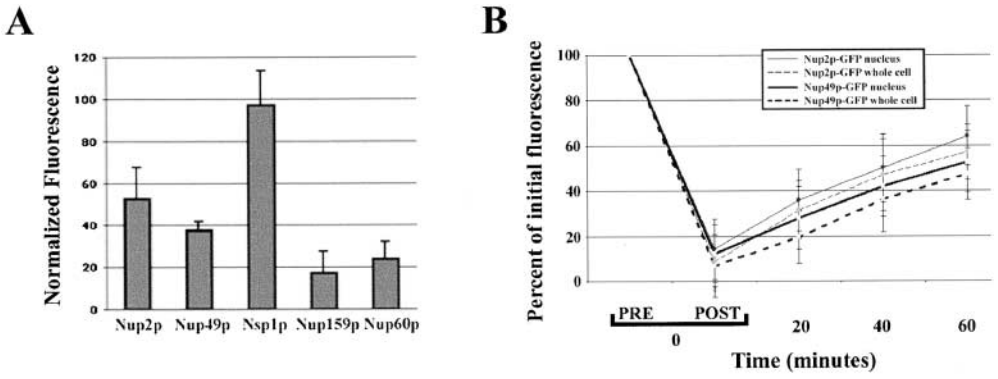

Figure 3. Nup2p–GFP and Nup49p–GFP expression levels and turnover rates are equivalent. (A) Relative nucleoporin levels quantified by analytical flow cytometry of GFP-tagged nucleoporins. Shown is a histogram of the background-normalized mean fluorescent intensity for Nup2p–GFP, Nup49p–GFP, Nsp1p–GFP, Nup60p–GFP, and Nup159p–GFP. These data establish that Nup2p–GFP and Nup49p–GFP are expressed at roughly equal levels with respect to other nucleoporins. Error bars represent the standard deviation over four independent experiments. (B) Quantitation of nucleoporin turnover rates using a photobleach/recovery assay. Nup2p–GFP or Nup49p–GFP-expressing cells were photobleached in an area encompassing the nucleus or the entire cell and then imaged at 20, 40, and 60 min after the photobleach. The average nuclear fluorescent intensity of bleached cells as a percentage of the initial fluorescence is plotted over time. Data points are the average of five cells, and the error bars represent the standard deviation. The recovery rate of Nup2p–GFP is equivalent to that of Nup49p–GFP and there was no significant difference between whole cell bleaching and bleaching of only the nuclear signal. Thus, the appearance of Nup2p–GFP in the recipient nucleus in heterokaryon experiments is due to movement of Nup2p–GFP rather than de novo protein synthesis or a cytoplasmic pool of Nup2p–GFP.

2000) and are thus in a position to provide a uniquely nuclear binding site for Nup2p. Immunopurification of Nup60p–pA yielded three proteins, identified by mass spectrometry as Kap60p, Kap95p, and Nup2p (Fig. 4 B). In contrast, immunopurification of Nup1p–pA yielded several proteins, including Kap95p and Kap60p but not Nup2p (data not shown). These data suggest that Nup60p is the nuclear site to which Nup2p binds.

As Nup2p interacts with both Kap60p and Kap95p in a trimeric complex, we also tested if Nup60p interacts directly with Kap60p and Kap95p by repeating the immunopurification of Nup60p–pA from a strain lacking Nup2p. In this case, we did not detect either Kap60p or Kap95p by Coomassie staining (data not shown) or by Western blotting using anti-Kap60p antibody (Fig. 4 C). These results suggest that, under these conditions, the interaction between Kap60p, Kap95p, and Nup60p is stabilized by Nup2p. Furthermore, altogether these data suggest that the Kap60p–Kap95p–Nup2p complex docks via Nup2p to Nup60p at the nucleoplasmic face of the NPC.

Deletion of NUP60 Results in Nuclear Accumulation of Nup2p–GFP and Kap60p–GFP

If Nup60p is at least partially responsible for the localization of Nup2p to the NPC, then loss or alteration of Nup60p should have a measurable effect on the subcellular distribution of Nup2p. We therefore observed the in vivo distribution of a Nup2p–GFP chimera in various different appropriate genetic backgrounds by fluorescence microscopy. In wild-type backgrounds, Nup2p–GFP chimeras displayed the punctate nuclear peripheral staining characteristic of a nucleoporin, and as with control nups, it clustered to one side of the NE in strains lacking Nup120p (Aitchison et al., 1995a; Heath et al., 1995; Rout et al., 2000) (Fig. 5, top). In agreement with our immunopurification results, deletion of *NUP1* (Belanger et al., 1994) had no obvious effect on the localization of Nup2p–GFP (Fig. 5, top). In contrast, deletion of *NUP60* caused Nup2p–GFP to accumulate in the nucleoplasm with a concomitant loss of concentration at the nuclear rim, whereas there appeared to be no effect on the control nucleoporins tested, Nsp1–GFP and Nup49p–GFP (Fig. 5, middle). Moreover, restoration of the expression of *NUP60* behind a galactose-inducible promoter returned Nup2p–GFP to its original location at the NPC (Fig. 5, bottom). Based on our immunopurification and fluorescence data, we conclude that Nup2p is tethered to the nuclear face of the NPC through its interaction with Nup60p.

One recently established role for Nup2p is in the efficient Cse1p-mediated export of Kap60p (Booth et al., 1999; Hood et al., 2000; Solsbacher et al., 2000). We therefore investigated if Nup60p is involved in the export of Kap60p. The distribution of Kap60p–GFP was monitored in strains lacking Nup60p or Nup2p and compared with wild-type cells, where Kap60p–GFP signal was detected throughout the cytoplasm and nucleoplasm but concentrated at the nuclear rim (Fig. 6). As shown, Kap60p–GFP accumulated in the nucleus in strains lacking Nup2p or Nup60p, but not in strains lacking the control nucleoporin Nup100p (see also Booth et al., 1999). We do note however that the Kap60p export defect in Δ*nup60* cells was not

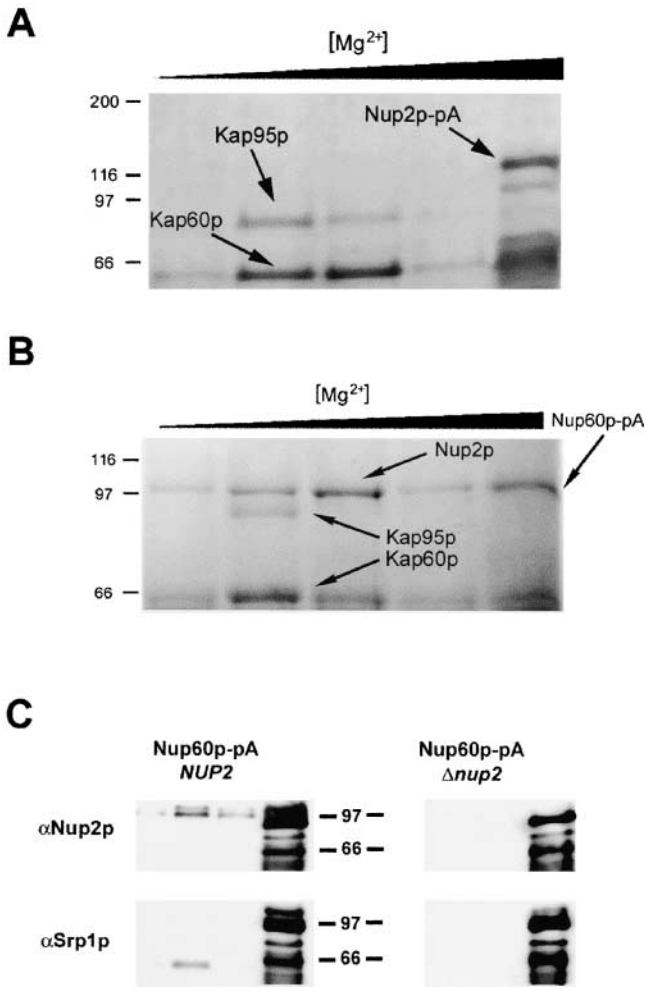

Figure 4. Nup2p docks at the NPC through an interaction with Nup60p and facilitates the formation of a tetrameric complex between Nup60p, Kap60p, Kap95p, and Nup2p. (A) Nup2p–pA from whole cell lysates was bound to IgG–Sepharose. Coprecipitating proteins were eluted with a $MgCl_2$ gradient, separated by SDS-PAGE, and detected by Coomassie blue staining. Shown, from left to right, are molecular mass standards (kD) followed by the fractions eluted by treatment with 0.2, 0.5, 1.0, 2.0, and 4.0 M $MgCl_2$. The two abundantly copurifying proteins were identified by mass spectrometry as Kap60p and Kap95p. No copurifying nucleoporins were detected. (B) Nup60p was immunoprecipitated from yeast whole cell lysates and analyzed as in A. Immunoprecipitation of Nup60p–pA from whole cell lysates coprecipitated Kap60p, Kap95p, and Nup2p, suggesting that Nup60p is the nucleoporin that anchors Nup2p to the nuclear face of the NPC. We detected no coprecipitating proteins by Coomassie staining when the same immunoprecipitation was performed from a strain lacking Nup2p (data not shown). (C) Immunoblot analysis of Nup60p–pA immunoprecipitations in wild-type and Δ*nup2* strains confirms the absence of both Nup2p and Kap60p in the Δ*nup2* strain. The 0.5, 1.0, 2.0, and 4.0 M $MgCl_2$ elution fractions from Nup60–pA immunoprecipitations in wild-type and Δ*nup2* strains were probed using anti-Kap60p (anti-SRP1) and anti-Nup2p antibodies. The absence of Kap60p in the immunoprecipitation from strains lacking Nup2p indicates that Nup2p facilitates the interaction between Nup60p and Kap60p and suggests that the interaction between Nup2p and Nup60p is direct. The two closely migrating bands recognized by the anti-Nup2p antibody are specific to Nup2p as neither band is present in strains lacking Nup2p. The signal observed in the 4,000 mM elution fraction represents Nup60–pA and Nup60p–pA breakdown products that bound to the rabbit polyclonal antibodies.

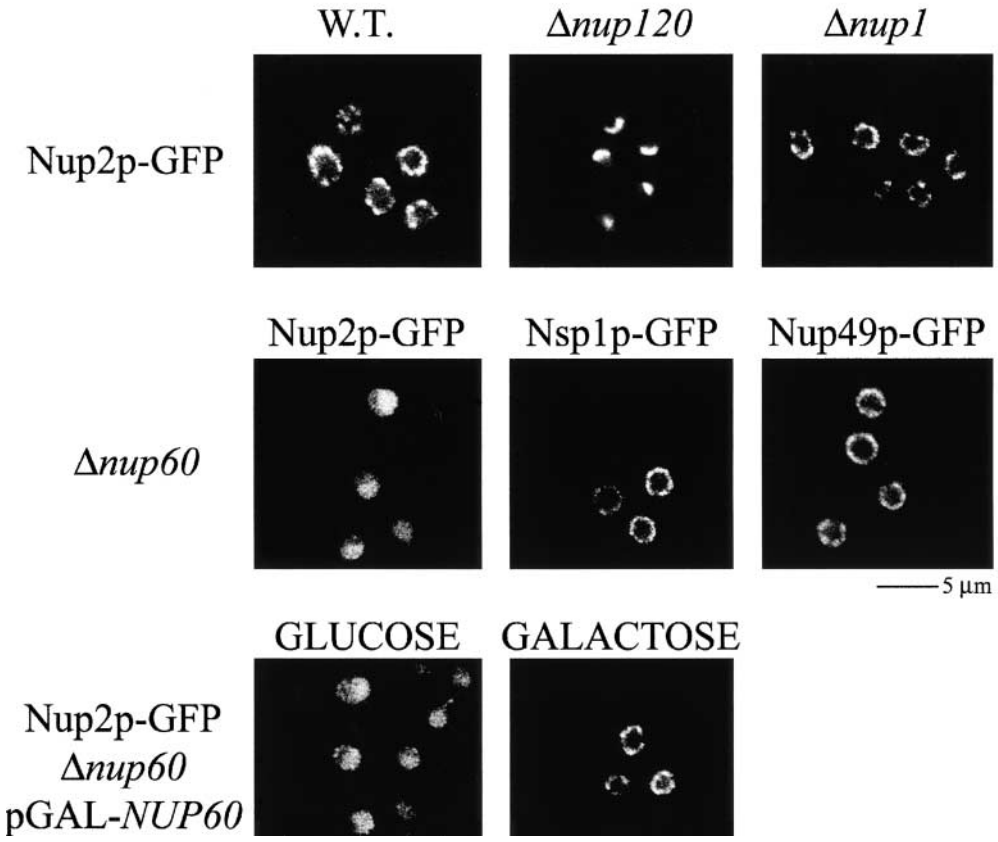

Figure 5. Nup60p facilitates the binding of Nup2p to the NPC. (Top) Nup2p–GFP in wild-type backgrounds exhibits punctate peripheral nuclear rim staining characteristic of a nucleoporin. Like other nucleoporins, Nup2p–GFP clusters to one face of the nuclear rim in cells lacking Nup120p. Consistent with our in vitro binding data, deletion of *NUP1* has no effect on the localization of Nup2p–GFP. (Middle) Deletion of *NUP60* results in the nuclear accumulation of Nup2p–GFP, but has no effect on the localization of the control nucleoporins, Nsp1p and Nup49p. (Bottom) In strains lacking Nup60p, Nup2p–GFP signal returned to the nuclear rim upon expression of *NUP60* from a galactose-inducible promoter.

as severe as that observed in Δ*nup2* cells, which suggests that Nup2p can support limited Kap60p export without interacting with Nup60p at the NPC and hints that Nup2p may also interact with other sites at the NPC.

This conclusion is also supported by genetic data. Cells lacking Nup2p or Nup60p grew normally and showed no temperature sensitivity (Loeb et al., 1993) (see below), whereas deletion of both *NUP60* and *NUP2* rendered cells inviable (Fig. 7 A). This genetic interaction demonstrates that, although Nup2p is mislocalized to the nucleoplasm in Δ*nup60* cells, it performs an essential function independent of its ability to interact with Nup60p at the NPC.

In light of the Kap60p export defect we observed in cells lacking Nup60p, we tested for a genetic interaction between *NUP60* and *KAP60*. Temperature-sensitive mutations of *KAP60* have previously been shown to be synthetically lethal with a deletion of *NUP2* (Booth et al., 1999). In contrast to Δ*nup2* cells, Δ*nup60* cells were not synthetically lethal with a temperature-sensitive mutation of *KAP60* (*srp1-31*), although they did exhibit greater temperature sensitivity as they failed to grow at 30°C (Fig. 7 B). This result is interesting because it also suggests that soluble nuclear Nup2p is partly functional. Furthermore, this lack of synthetic lethality agrees with our fluorescence data, which suggests deletion of *NUP2* has a more severe effect on Kap60p export than deletion of *NUP60*. These data confirm that Nup60p is required for the efficient export of Kap60p, and that the function of Nup2p in Kap60p export is compromised (but not completely abrogated) when unable to interact with the NPC through Nup60p.

The RBD of Nup2p Is Important for Nup2p Function and Localization to the NPC

Nup2p can be divided into three distinct domains. The NH_2-terminal 172 amino acids are responsible for interaction with both Kap60p and the NPC (Booth et al., 1999; Hood et al., 2000). The central domain (amino acids 182–546) contains several FXFG repeats typical of domains found in other nucleoporins that bind to members of the Kap superfamily. The COOH terminus (amino acid residues 556–720) contains a RBD, homologous to the RBD of the shuttling protein, Ran binding protein 1 (Yrb1p in yeast) (Hartmann et al., 1994; Dingwall et al., 1995; Kunzler et al., 2000), the yeast nuclear protein Yrb2p, and the cytoplasmically disposed mammalian nucleoporin Nup358 (Wu et al., 1995). Although the RBD of Nup2p has been shown to bind Ran (Dingwall et al., 1995), no other function has been attributed to this domain. We therefore investigated if the RBD of Nup2p is required to rescue the lethal phenotype observed in cells lacking both Nup2p and Nup60p (Fig. 7 C). Interestingly, transformation of a plasmid encoding only residues 1–546 of Nup2p, lacking the RBD (Nup2ΔRBD; pLDB690) was unable to fully compensate for the loss of Nup2p in this strain. Cells expressing Nup2ΔRBD grew normally at 30°C but failed to grow at 37°C, demonstrating that the RBD contributes to efficient Nup2p function. These results agree with the previously reported observation that the Kap60p export defect observed in Δ*nup2* null cells is only partly rescued by Nup2p mutants lacking the RBD (Booth et al., 1999).

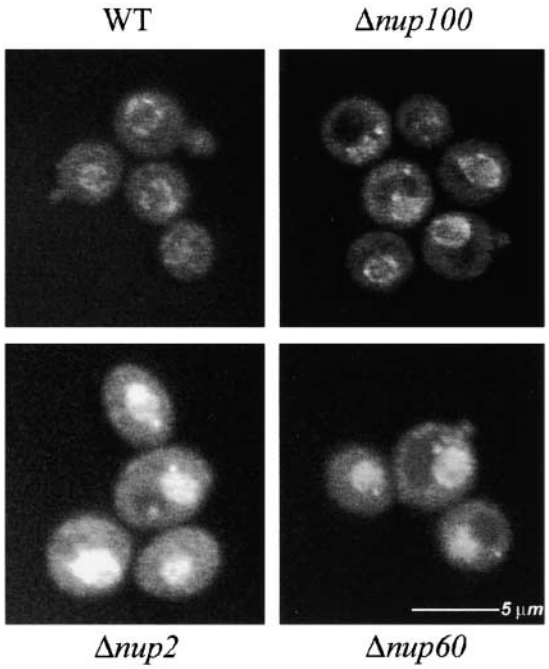

Figure 6. Nup60p is involved in the export of Kap60p from the nucleus. In agreement with previous reports, we observed a nuclear accumulation of Kap60p–GFP in cells lacking Nup2p. This defect was also observed, but was less severe, in strains lacking Nup60p, which suggests that Nup2p docking to Nup60p plays a role in Cse1p-mediated export of Kap60p. The localization of Kap60p–GFP was unaffected by deletion of *NUP100*, indicating that the redistribution observed in cells lacking Nup2p or Nup60p is specific.

The observation that the RBD of Nup2p is required for efficient Nup2p function suggests that this domain may also be important for its movement or tethering to the NPC. We created a genomic integration of Nup2ΔRBD–GFP (Nup2p residues 1–605 carrying a COOH-terminal fusion to GFP) and monitored the distribution of this Nup2p chimera in an otherwise wild-type background. Indeed, although this mutant contains the NPC-interacting domain (Hood et al., 2000), fluorescence microscopy revealed that there was a substantial increase in the nuclear proportion of Nup2p in the absence of its RBD (Fig. 8, top). Quantitation of GFP fluorescence along nuclear bisects was performed for Nup2p–GFP in wild-type and Δ*nup60* backgrounds and compared with Nup2ΔRBD–GFP distribution (Fig. 8, bottom). These profile plots indicate that the steady-state localization of the Nup2ΔRBD–GFP mutant is shifted to the nucleus, although this mutant retains its ability to interact with the NPC. These data support a model in which the RBD of Nup2p contributes to its interaction with the NPC, perhaps by modulating its ability to bind to either Nup60p at the nuclear face or another nucleoporin at the cytoplasmic face.

Nup2p Docks to an Alternative Site in the NPC When Transport Is Inhibited

To further explore the role of Ran in the association of Nup2p with the NPC, we tested if perturbations in the Ran cycle could alter the distribution of Nup2p in vivo by two methods. First, cells were metabolically poisoned by treatment with sodium azide and deoxyglucose (Fig. 9 A, i). Azide/deoxyglucose treatment is believed to inhibit nuclear transport by decreasing ATP levels, thereby affecting GTP levels (Shulga et al., 1996). In the second method, Ran-GTP pools were depleted by temperature shift of cells carrying a mutation in the Ran-GTP exchange factor *PRP20* (Fig. 9 A, ii) (Amberg et al., 1993). Neither of these stresses affected the localization of control nucleoporins (data not shown) or Nup2p–GFP in a wild-type background. Interestingly, when Nup2p–GFP was monitored in Δ*nup60* background, both conditions led to a shift of the Nup2p–GFP from the nucleoplasm to the nuclear rim. Similarly, Kap60p–GFP accumulated at the nuclear rim, indicating a block in nuclear transport. Thus, it is likely that another site within the NPC serves to dock Nup2p under conditions where Ran-GTP levels are low and/or transport is inactive. Our IEM data suggest that this alternative docking site is at the cytoplasmic face of the NPC. Indeed, we repeated this immunoelectron microscopic localization of Nup2p–pA in nuclei lacking Nup60p and found Nup2p–pA concentrated on the cytoplasmic face of the NPC. This would explain why the localization of Nup2p–GFP appeared unaffected by Ran perturbations in wild-type cells, as fluorescence microscopy would not detect a relocalization of Nup2p–GFP from the nuclear to the cytoplasmic face of the NPC. Studies are currently underway to identify this second Nup2p binding site.

Discussion

The yeast NPC contains ~30 nucleoporins, defined by their stable contributions to the overall structure (Rout et al., 2000). Nucleoporins, in turn, interact with numerous transport factors that dock transiently to the NPC to mediate the translocation of cargoes across the NE. We and others have attempted to understand this process by identifying all the players involved in nucleocytoplasmic transport and characterizing the dynamics of the interactions between nucleoporins and transport factors. By most criteria, Nup2p resembles a typical yeast nucleoporin: it contains FG repeats, exhibits punctate peripheral nuclear rim staining by fluorescence microscopy, genetically interacts with other nucleoporins, and is present in biochemical fractions enriched in NPCs. These characteristics, though, are not limited to static components of the NPC, and careful examination of the localization and dynamics of proteins that harbor these attributes has led to novel insights into their functions. For example, because of its concentration at the NPC and its genetic interactions with nucleoporins, the cNLS receptor, Kap60p/Srp1p was originally characterized as an NPC component (Belanger et al., 1994). Also, Kap123p, a kap responsible for importing ribosomal proteins, was identified as a major protein within the isolated highly enriched NPC fraction, and it too yields punctate peripheral NPC-like staining (Rout et al., 1997). However, further characterization of these and other transport factors has since demonstrated that members of this class of proteins are present in the cytoplasm and nucleoplasm, and thus their staining patterns reflect an observed dynamic presence at the NPC. Furthermore, Yrb2p, like Nup2p, contains FG repeats and, on this basis, an RBD and was originally classified as a nucleoporin

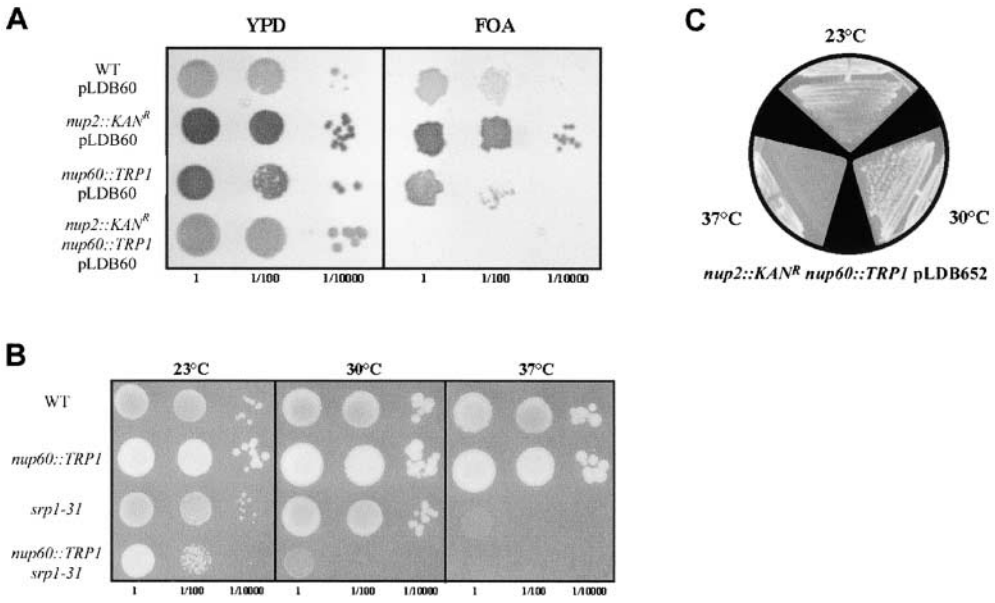

Figure 7. Genetic interactions between *NUP2*, *NUP60*, and *KAP60*. (A) Δ*nup2* and Δ*nup60* strains were crossed and sporulated with the covering plasmid, pLDB60 (*NUP2 URA3 CEN*). Progeny of the indicated genotypes were assayed for the ability to grow without the *NUP2*-covering plasmid by growth on fluoroorotic acid. As shown by serial dilution of logarithmically growing cultures, only the double mutant fails to grow on fluororotic acid, indicating that *NUP2* and *NUP60* are synthetically lethal. (B) To assess any genetic interaction between *NUP60* and *KAP60*, we mated a strain harboring a temperature-sensitive *KAP60* allele, *srp1-31*, with a *nup60* null strain. Wild-type and single and double mutant spores were isolated and assayed for their ability to grow at 23°C, 30°C, and 37°C. A genetic interaction was observed between *KAP60* and *NUP60*, as the Δ*nup60,srp1-31* strain failed to grow at 30°C, whereas the *srp1-31* single mutant grew at 30°C but not at 37°C. (C) Expression of a Nup2p mutant lacking the RBD of Nup2p rescues the synthetic lethality observed between *Nup2* and *Nup60*, but conveys a temperature-sensitive phenotype. A plasmid encoding amino acid residues 1–546 of Nup2p (pLDB690) was able to partially rescue the synthetic lethality observed between *NUP2* and *NUP60*. Δ*nup2*,Δ*nup60* cells carrying the pLDB690 plasmid grew slowly at 23°C and normal at 30°C, but failed to grow at 37°C. Thus, the RBD of Nup2p performs a function that becomes essential in strains lacking Nup60p.

(Nehrbass and Blobel, 1996). More detailed examination of Yrb2p determined that it is a soluble nuclear protein, and this information was used to establish a novel role for Yrb2p in NES-mediated export (Taura et al., 1997, 1998).

Similarly, although Nup2p was originally defined as a nucleoporin, we recently excluded it as a bona fide nucleoporin based on its failure to enrich with purified NEs and its partial presence in the nucleoplasm and cytosol (Aitchi-

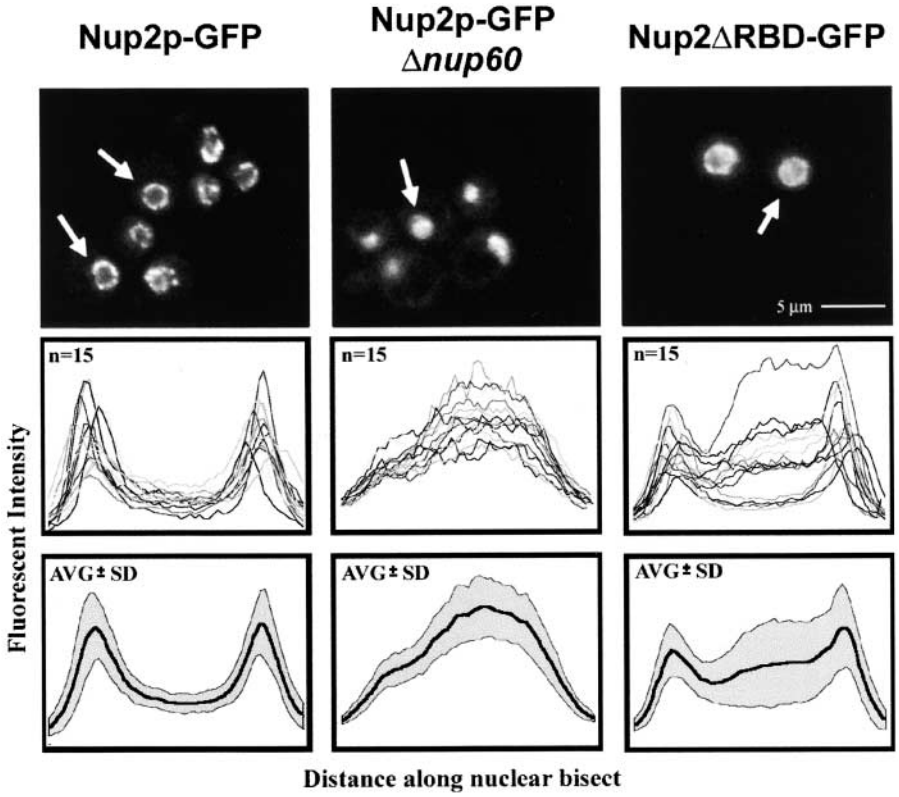

Figure 8. Deletion of the RBD of Nup2p affects its ability to bind to the NPC. (Top) Images of Nup2p–GFP in wild-type and Δ*nup60* cells as well as for Nup2ΔRBDp–GFP in an otherwise wild-type background. (Middle) Plots of the fluorescent intensity across a nuclear bisect for 15 cells, each of the strains above. (Bottom) Plots of the mean (thick line) and standard deviation (shaded region) of data presented above. Comparison reveals an increased nuclear signal of Nup2ΔRBDp–GFP relative to Nup2p–GFP. However, relative to Nup2p–GFP in strains lacking Nup60p, there remained a significant portion of Nup2ΔRBDp–GFP present at the nuclear rim.

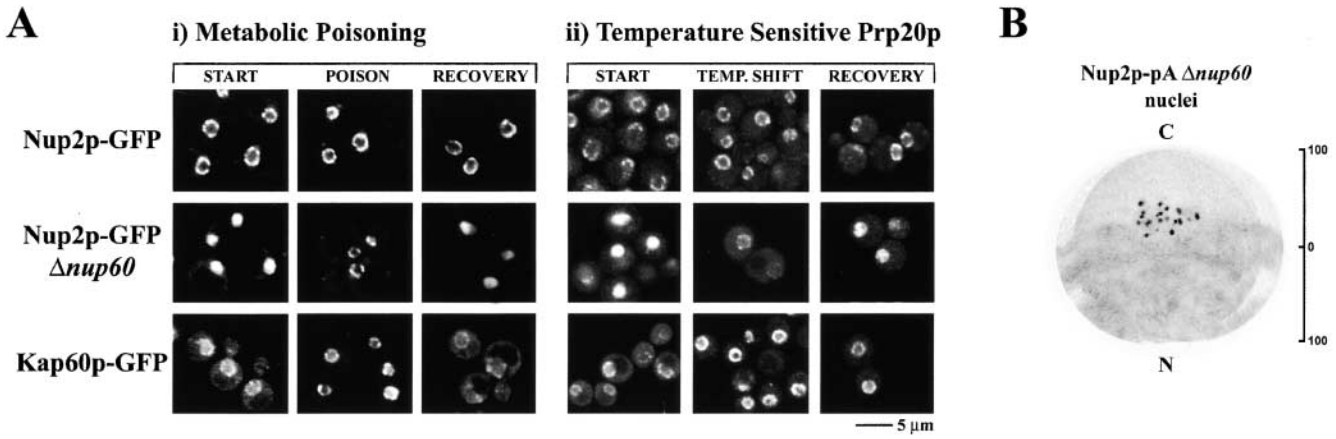

Figure 9. Perturbations in the Ran cycle can return Nup2p–GFP to the NPC in strains lacking Nup60p. (Ai) After initial image acquisition (START), the indicated strains were metabolically poisoned by azide/deoxyglucose treatment for 45 min (POISON). No change in the localization of Nup2p–GFP was observed. In contrast, Nup2p–GFP accumulated at the nuclear rim in strains lacking Nup60p after the 45-min poisoning treatment. The localization of Kap60p–GFP similarly accumulated at the nuclear rim under these conditions. Furthermore, a 10-min recovery period in glucose-containing media resulted in the return of Nup2p–GFP and Kap60p–GFP to their respective steady-state locales (RECOVERY). (Aii) Inactivation of the Ran-GTP exchange factor, Prp20p, enhances binding of Nup2p to alternative sites within the NPC. Nup2p–GFP was expressed in Δ*nup60*,*prp20-7* cells, grown at 23°C (START), shifted to 37°C for 90 min (TEMP. SHIFT), and then recovered at room temperature for 60 min (RECOVERY). Kap60p–GFP accumulated at the nuclear rim at the nonpermissive temperature, indicating a block in nuclear transport. Neither Nup49p–GFP nor Nup2p–GFP in otherwise wild-type cells appeared affected by this treatment; however, Nup2p–GFP signal returned to the nuclear rim and accumulated in the cytoplasm in a strain lacking Nup60p. This effect was reversible as growth at the permissive temperature restored the steady-state nuclear localization of Nup2p–GFP in the Δ*nup60* strain. (B) The alternative NPC docking site of Nup2p is likely at the cytoplasmic face of the NPC. Nup2p–pA in cells lacking Nup60p was localized by IEM of purified nuclei. We could find no signal was detected on the nuclear face of the NPC; however, there remained a pool of Nup2p–pA that remained associated with the NPC on the cytoplasmic face.

son et al., 1996; Rout et al., 2000, 1997). In this study, we focussed on answering two fundamental questions: is Nup2p a stable component of the NPC and, if not, how is its dynamic connection to the NPC mediated? To answer the first question, we exploited the *kar1-1* mutant to create yeast heterokaryons and monitored the ability of GFP fusions of Nup2p and control nucleoporins to illuminate the unlabeled NPCs. In this assay, only Nup2p transferred rapidly from the original nucleus to the second nucleus, demonstrating that Nup2p is indeed mobile and is capable of entering the soluble phase of nucleocytoplasmic transport. Interestingly however, in these experiments, Nup2p did not move as rapidly as the kaps, Kap60p, or Cse1p (data not shown). This suggests that Nup2p did not freely equilibrate between the two nuclei in the heterokaryon experiments, rather, that in vivo it escapes the vicinity of the NPC at a relatively low rate, at which time it is capable of diffusing through the cytoplasm and moving to the recipient NPC.

To address how Nup2p is tethered to the NPC, we immunopurified pA chimeras and showed that Nup2p binds in a complex with Kap95p and Kap60p, which together interact at the nuclear face of NPC through Nup60p. In support of these in vitro binding studies, we showed that deletion of *NUP60* led to a shift of the steady-state localization of Nup2p from the NPC primarily to the nucleoplasm, but also to a lesser extent to the cytoplasm. In addition, the absence of Nup60p led to a defect in Kap60p export. Others have recently provided evidence that Nup2p interacts directly with Kap60p and acts as a scaffold in the formation of a trimeric export complex between Cse1p, Kap60p, and Ran-GTP (Booth et al., 1999; Hood et al., 2000; Solsbacher et al., 2000). Given the nature of the complex formed, it is likely these reactions occur at the nucleoplasmic side of the NPC. Our results support this model, and demonstrate that the previously observed interaction between the NH_2-terminal region of Nup2p and the NPC (Hood et al., 2000) is through the nucleoplasmically disposed nucleoporin, Nup60p. Furthermore, genetic and fluorescence microscopy evidence presented here demonstrate that the interaction between Nup2p and Nup60p facilitates, but is not required for, efficient Kap60p export. Moreover, because we were able to isolate a complex between Nup60p, Nup2p, Kap60p, and Kap95p, it is likely that the Kap60p and NPC binding domains are distinct.

In addition to localizing Nup2p to the nuclear side of the NPC and observing a strong interaction between Nup2p with Nup60p, we detected a significant fraction of Nup2p in the nucleoplasm and bound to the cytoplasmic face of the NPC. This observation supports the idea that Nup2p is mobile, shuttling between different sides of the NPC. Nevertheless, it appears that Nup2p binds most avidly to Nup60p in the normal cellular environment and spends little time on the cytoplasmic side. This is based primarily on two pieces of data. First, deletion of *NUP60* causes the majority of Nup2p to lose its interaction with the NPC. Second, electron microscopy of fixed whole cells shows that the majority of Nup2p is localized to the distal nuclear regions of the NPC (Hood et al., 2000; Solsbacher et al., 2000). Therefore, to understand the movement of Nup2p, we asked what conditions promote the movement of Nup2p away from the nuclear face of the NPC. Because of the central role that Ran plays in conferring the directional movement of transport factors, we deleted the RBD of Nup2p and altered the GTP-bound state of Ran in or-

der to determine if these changes influenced the subcellular distribution of Nup2p. Deletion of the RBD from the COOH terminus of Nup2p shifted the equilibrium of Nup2p to the nucleoplasm. Second, when *NUP60* was deleted, Nup2p returned to the NPC when ATP or Ran-GTP concentrations were depleted by metabolic poisoning or by mutations of the Ran cycle, respectively. These data suggest that Ran-GTP strengthens the interaction between Nup2p and Nup60p. Furthermore, they suggest that Nup2p moves in response to the absence of Ran-GTP or, as domains homologous to the RBD of Nup2p bind both nucleotide-bound forms of Ran, in association with Ran-GDP. This may explain why Nup2p was not found at the cytoplasmic side of the NPC by IEM of whole cells. In wild-type growing cells, Nup2p may be only transiently associated with the cytoplasmic face; a high availability of Ran-GTP would favor Nup2p's interaction with Nup60p. However, during the isolation of nuclei, Ran-GTP would be depleted, thereby shifting Nup2p's equilibrium and serendipitously allowing us to visualize it at the cytoplasmic face. However, it appears that although the interaction between Nup60p and Nup2p is strengthened by Ran-GTP, Ran-GTP is not required for this binding because we readily observe this complex by various means in vitro.

Nup2p, like many other components of the nucleocytoplasmic transport machinery, is not essential, but increases the efficiency of transport (Loeb et al., 1993; Booth et al., 1999; Hood et al., 2000; Solsbacher et al., 2000). We previously suggested that nucleoporins asymmetrically positioned on one side of the NPC provide a high affinity binding site for transport complexes, thereby enhancing the directionality of movement across the NPC (Rout et al., 2000). Again, the binding sites provided by these nucleoporins are not essential but increase the efficiency of transport (Belanger et al., 1994; Del Priore et al., 1997; Saavedra et al., 1997) (Fig. 6). In the case of the Kap95p–Kap60p–cNLS import complex, we believe that the nucleoporin contributing to directional movement through the NPC is Nup1p. This is based on our observations that Nup1p is an asymmetric nuclear-disposed nucleoporin (Rout et al., 2000) and is the most stably bound nucleoporin in Kap95p–pA immunopurifications (unpublished data). Nup2p also binds avidly to Kap95p–pA, but does so within soluble subcellular fractions (Aitchison et al., 1996; Rout et al., 1997). Together, we suggest that upon import, the Kap95p–Kap60p complex moves preferentially to Nup1p at the nuclear side of the NPC. Once bound to this site, efficient transport is maintained by transferring the complex to the mobile factor Nup2p, which can enter the nucleoplasm. The constant removal of Kap60p and Kap95p from Nup1p by Nup2p would enhance transport by moving the products of the transport reaction away from the NPC. Kap95p (and perhaps cargo) would be released from Nup2p by the transfer of Ran-GTP to Kap95p. This transfer may also be facilitated by the ability of Nup2p to interact simultaneously with both Kap95p and Ran-GTP. Kap60p would remain bound to Nup2p, and the Kap60p–Cse1p–Ran-GTP export complex would form on Nup2p, which may then return to the NPC, likely by binding to Nup60p.

At this time, we have not elucidated a role for Nup2p in the cytoplasm. In mammalian cells, Ran binds to nucleoporins present on both the cytoplasmic and nucleoplasmic faces of the NPC. As none of the yeast nucleoporins contain RBDs, the cytoplasmically disposed Nup2p may perform functions analogous to the cytoplasmic mammalian nucleoporin Nup358. Nup358 binds Ran-GDP and Ran-GTP through its multiple RBDs, whereas a separate Zn-finger motif binds to Ran-GDP (Yaseen and Blobel, 1999b). Like Nup2p, Nup358 also contains FG repeats for binding to kaps and has been proposed to act at the cytoplasmic face as a molecular scaffold for the recycling of the Kap95p orthologue, Kapβ1, by coordinating Ran-GTP hydrolysis with the termination and reinitiation of each transport cycle (Yaseen and Blobel, 1999a).

It is also possible that the mobility of Nup2p plays a more direct role in the Ran cycle and transport. Although the asymmetric distribution of Ran-GTP and Ran-GDP is central to current models of transport, it remains unknown to what extent Ran is active in the NPC itself, and to what extent it modulates specific reactions between transport factors and individual nucleoporins. Recent results demonstrate that the mammalian homologue of Prp20p, RCC1, although thought to be restricted to the nucleus, is also present on the cytoplasmic surface of the NPC (Fontoura et al., 2000). Furthermore, Rna1p is not restricted to the cytoplasm, as it is observed in the nucleoplasm in yeast (Traglia et al., 1996). In addition, RanBP1, a protein proposed to augment Rna1p's Ran-GAP activity in the cytoplasm, also shuttles between the nucleus and cytoplasm (Kunzler et al., 2000). Thus, although it is virtually certain that there exists a steep Ran-GDP versus Ran-GTP gradient across the NE, modifiers of the nucleotide-bound state of Ran exist on both sides of the NPC. Given that Nup2p exhibits genetic interactions with Prp20p (Booth et al., 1999), perhaps Nup2p is involved in the regulation of Ran in the vicinity of the NPC.

Interestingly, a potential mammalian orthologue of Nup2p has recently been characterized. Nup50, originally termed Npap60, contains a RBD and FG repeats and localizes to the nuclear face of the NPC (Fan et al., 1997; Guan et al., 2000; Smitherman et al., 2000). The localization of Nup50 to the region near Nup153 by IEM and in vitro binding data suggests that Nup153 may perform a function similar to the role of Nup60p in yeast by docking Nup50 at the NPC (Guan et al., 2000). Like Nup2p, Nup50 exhibits many characteristics not typical of bona fide nucleoporins, such as fixation-dependent localization by immunofluorescence and variable expression and localization at different stages of the cell cycle and in different cell types (Guan et al., 2000; Smitherman et al., 2000). It will be interesting to see if this potential Nup2p orthologue is also a mobile nucleoporin that cycles on and off the NPC in a Ran-dependent manner.

We thank Helen Shio and the Rockefeller University Electron Microscopy Facility for outstanding and dedicated support; the University of Alberta Confocal Microscopy Facility; Dwayne Weber for expert technical assistance; and Nataliya Shulga, Laura Davis, Kenneth Belanger, Susan Wente, and Charles Cole for gifts of yeast strains and plasmids. We also thank Rowan Christmas and Kerry Deutsch for help with computer analyses, Marcello Marelli for critical reading of the manuscript, other members of the Aitchison laboratory for helpful discussion, and anonymous reviewers for constructive input.

This research was supported by operating and salary support from The

Medical Research Council of Canada/Canadian Institute for Health Research and Alberta Heritage Foundation for Medical Research to J.D. Aitchison, D.J. Dilworth, and R.W. Wozniak; The Institute for Systems Biology to J.D. Aitchison; The Howard Hughes Medical Institute to A. Suprapto; the Rita Allen, Sinsheimer, and Hirschl Foundations and The Rockefeller University to M.P. Rout; and The National Institutes of Health (grant RR 00862) to B.T. Chait.

Submitted: 31 January 2001
Revised: 17 April 2001
Accepted: 19 April 2001

References

Aitchison, J.D., G. Blobel, and M.P. Rout. 1995a. Nup120p: a yeast nucleoporin required for NPC distribution and mRNA transport. *J. Cell Biol.* 131:1659–7165.

Aitchison, J.D., M.P. Rout, M. Marelli, G. Blobel, and R.W. Wozniak. 1995b. Two novel related yeast nucleoporins Nup170p and Nup157p: complementation with the vertebrate homologue Nup155p and functional interactions with the yeast nuclear pore-membrane protein Pom152p. *J. Cell Biol*. 131: 1133–1148.

Aitchison, J.D., G. Blobel, and M.P. Rout. 1996. Kap104p: a karyopherin involved in the nuclear transport of messenger RNA binding proteins. *Science*. 274:624–627.

Akey, C.W. 1995. Structural plasticity of the nuclear pore complex. *J. Mol. Biol.* 248:273–293.

Allen, T.D., J.M. Cronshaw, S. Bagley, E. Kiseleva, and M.W. Goldberg. 2000. The nuclear pore complex: mediator of translocation between nucleus and cytoplasm. *J. Cell Sci*. 113:1651–1659.

Amberg, D.C., M. Fleischmann, I. Stagljar, C.N. Cole, and M. Aebi. 1993. Nuclear PRP20 protein is required for mRNA export. *EMBO J*. 12:233–241.

Bayliss, R., T. Littlewood, and M. Stewart. 2000. Structural basis for the interaction between FxFG nucleoporin repeats and importin-β in nuclear trafficking. *Cell*. 102:99–108.

Belanger, K.D., M.A. Kenna, S. Wei, and L.I. Davis. 1994. Genetic and physical interactions between Srp1p and nuclear pore complex proteins Nup1p and Nup2p. *J. Cell Biol*. 126:619–630.

Blobel, G. 1995. Unidirectional and bidirectional protein traffic across membranes. *Cold Spring Harb. Symp. Quant. Biol*. 60:1–10.

Booth, J.W., K.D. Belanger, M.I. Sannella, and L.I. Davis. 1999. The yeast nucleoporin Nup2p is involved in nuclear export of importin α/Srp1p. *J. Biol. Chem*. 274:32360–32367.

Bucci, M., and S.R. Wente. 1997. In vivo dynamics of nuclear pore complexes in yeast. *J. Cell Biol*. 136:1185–1199.

Cole, C.N., and C.M. Hammell. 1998. Nucleocytoplasmic transport: driving and directing transport. *Curr. Biol*. 8:R368–R372.

Conti, E., M. Uy, L. Leighton, G. Blobel, and J. Kuriyan. 1998. Crystallographic analysis of the recognition of a nuclear localization signal by the nuclear import factor karyopherin α. *Cell*. 94:193–204.

Damelin, M., and P.A. Silver. 2000. Mapping interactions between nuclear transport factors in living cells reveals pathways through the nuclear pore complex. *Mol. Cell*. 5:133–140.

Del Priore, V., C. Heath, C. Snay, A. MacMillan, L. Gorsch, S. Dagher, and C. Cole. 1997. A structure/function analysis of Rat7p/Nup159p, an essential nucleoporin of *Saccharomyces cerevisiae*. *J. Cell Sci*. 110:2987–2999.

Dingwall, C., S. Kandels-Lewis, and B. Seraphin. 1995. A family of Ran binding proteins that includes nucleoporins. *Proc. Natl. Acad. Sci. USA*. 92:7525–7529.

Fan, F., C.P. Liu, O. Korobova, C. Heyting, H.H. Offenberg, G. Trump, and N. Arnheim. 1997. cDNA cloning and characterization of Npap60: a novel rat nuclear pore-associated protein with an unusual subcellular localization during male germ cell differentiation. *Genomics*. 40:444–453.

Fontoura, B.M., G. Blobel, and N.R. Yaseen. 2000. The nucleoporin Nup98 is a site for GDP/GTP exchange on ran and termination of karyopherin β 2-mediated nuclear import. *J. Biol. Chem*. 275:31289–31296.

Fornerod, M., M. Ohno, M. Yoshida, and I.W. Mattaj. 1997. CRM1 is an export receptor for leucine-rich nuclear export signals. *Cell*. 90:1051–1060.

Gorlich, D., N. Pante, U. Kutay, U. Aebi, and F.R. Bischoff. 1996. Identification of different roles for RanGDP and RanGTP in nuclear protein import. *EMBO J*. 15:5584–5594.

Görlich, D., and V. Kutay. 1999. Transport between the cell nucleus and the cytoplasm. *Annu. Rev. Cell. Dev. Biol.* 15:607–660.

Guan, T., R.H. Kehlenbach, E.C. Schirmer, A. Kehlenbach, F. Fan, B.E. Clurman, N. Arnheim, and L. Gerace. 2000. Nup50, a nucleoplasmically oriented nucleoporin with a role in nuclear protein export. *Mol. Cell. Biol*. 20:5619–5630.

Hartmann, E., T. Sommer, S. Prehn, D. Gorlich, S. Jentsch, and T.A. Rapoport. 1994. Evolutionary conservation of components of the protein translocation complex. *Nature*. 367:654–657.

Heath, C.V., C.S. Copeland, D.C. Amberg, V. Del Priore, M. Snyder, and C.N. Cole. 1995. Nuclear pore complex clustering and nuclear accumulation of poly(A)$^+$ RNA associated with mutation of the *Saccharomyces cerevisiae* RAT2/NUP120 gene. *J. Cell Biol*. 131:1677–1697.

Hood, J.K., J.M. Casolari, and P.A. Silver. 2000. Nup2p is located on the nuclear side of the nuclear pore complex and coordinates Srp1p/importin-α export. *J. Cell Sci*. 113:1471–1480.

Kehlenbach, R.H., A. Dickmanns, A. Kehlenbach, T. Guan, and L. Gerace. 1999. A role for RanBP1 in the release of CRM1 from the nuclear pore complex in a terminal step of nuclear export. *J. Cell Biol*. 145:645–657.

King, M.G., and D.G. Baskin. 1991. Effect of paraformaldehyde fixation on localization and characterization of insulin-like growth factor-I (IGF-I) receptors in the rat brain. *Anat. Rec*. 231:467–472.

Kraemer, D.M., C. Strambio-de-Castillia, G. Blobel, and M.P. Rout. 1995. The essential yeast nucleoporin NUP159 is located on the cytoplasmic side of the nuclear pore complex and serves in karyopherin-mediated binding of transport substrate. *J. Biol. Chem*. 270:19017–19021.

Kunzler, M., T. Gerstberger, F. Stutz, F.R. Bischoff, and E. Hurt. 2000. Yeast Ran-binding protein 1 (Yrb1) shuttles between the nucleus and cytoplasm and is exported from the nucleus via a CRM1 (XPO1)-dependent pathway. *Mol. Cell. Biol*. 20:4295–4308.

Loeb, J.D., L.I. Davis, and G.R. Fink. 1993. NUP2, a novel yeast nucleoporin, has functional overlap with other proteins of the nuclear pore complex. *Mol. Biol. Cell*. 4:209–222.

Marelli, M., J.D. Aitchison, and R.W. Wozniak. 1998. Specific binding of the karyopherin Kap121p to a subunit of the nuclear pore complex containing Nup53p, Nup59p, and Nup170p. *J. Cell Biol*. 143:1813–1830.

Mattaj, I.W., and L. Englmeier. 1998. Nucleocytoplasmic transport: the soluble phase. *Annu. Rev. Biochem*. 67:265–306.

Moore, M.S. 1998. Ran and nuclear transport. *J. Biol. Chem*. 273:22857–22860.

Murphy, R., J.L. Watkins, and S.R. Wente. 1996. GLE2, a *Saccharomyces cerevisiae* homologue of the *Schizosaccharomyces pombe* export factor RAE1, is required for nuclear pore complex structure and function. *Mol. Biol. Cell*. 7:1921–1937.

Nehrbass, U., and G. Blobel. 1996. Role of the nuclear transport factor p10 in nuclear import. *Science*. 272:120–122.

Nehrbass, U., M.P. Rout, S. Maguire, G. Blobel, and R.W. Wozniak. 1996. The yeast nucleoporin Nup188p interacts genetically and physically with the core structures of the nuclear pore complex. *J. Cell Biol*. 133:1153–1162.

Pemberton, L.F., G. Blobel, and J.S. Rosenblum. 1998. Transport routes through the nuclear pore complex. *Curr. Opin. Cell Biol*. 10:392–399.

Rexach, M., and G. Blobel. 1995. Protein import into nuclei: association and dissociation reactions involving transport substrate, transport factors, and nucleoporins. *Cell*. 83:683–692.

Rout, M.P., and J.D. Aitchison. 2001. The nulcear pore complex as a transport machine. *J. Biol. Chem.* 276:16593–16596.

Rout, M.P., J.D. Aitchison, A. Suprapto, K. Hjertaas, Y. Zhao, and B.T. Chait. 2000. The yeast nuclear pore complex: composition, architecture, and transport mechanism. *J. Cell Biol*. 148:635–651.

Rout, M.P., and G. Blobel. 1993. Isolation of the yeast nuclear pore complex. *J. Cell Biol*. 123:771–783.

Rout, M.P., G. Blobel, and J.D. Aitchison. 1997. A distinct nuclear import pathway used by ribosomal proteins. *Cell*. 89:715–725.

Ryan, K.J., and S.R. Wente. 2000. The nuclear pore complex: a protein machine bridging the nucleus and cytoplasm. *Curr. Opin. Cell Biol*. 12:361–371.

Saavedra, C.A., C.M. Hammell, C.V. Heath, and C.N. Cole. 1997. Yeast heat shock mRNAs are exported through a distinct pathway defined by Rip1p. *Genes Dev*. 11:2845–2856.

Shulga, N., P. Roberts, Z. Gu, L. Spitz, M.M. Tabb, M. Nomura, and D.S. Goldfarb. 1996. In vivo nuclear transport kinetics in *Saccharomyces cerevisiae*: a role for heat shock protein 70 during targeting and translocation. *J. Cell Biol*. 135:329–339.

Smitherman, M., K. Lee, J. Swanger, R. Kapur, and B.E. Clurman. 2000. Characterization and targeted disruption of murine Nup50, a p27(Kip1)-interacting component of the nuclear pore complex. *Mol. Cell. Biol*. 20:5631–5642.

Solsbacher, J., P. Maurer, F. Vogel, and G. Schlenstedt. 2000. Nup2p, a yeast nucleoporin, functions in bidirectional transport of importin α. *Mol. Cell. Biol*. 20:8468–8479.

Stade, K., C.S. Ford, C. Guthrie, and K. Weis. 1997. Exportin 1 (Crm1p) is an essential nuclear export factor. *Cell*. 90:1041–1050.

Stoffler, D., B. Fahrenkrog, and U. Aebi. 1999. The nuclear pore complex: from molecular architecture to functional dynamics. *Curr. Opin. Cell Biol*. 11:391–401.

Strambio-de-Castillia, C., G. Blobel, and M.P. Rout. 1999. Proteins connecting the nuclear pore complex with the nuclear interior. *J. Cell Biol*. 144:839–855.

Taura, T., G. Schlenstedt, and P.A. Silver. 1997. Yrb2p is a nuclear protein that interacts with Prp20p, a yeast Rcc1 homologue. *J. Biol. Chem*. 272:31877–31884.

Taura, T., H. Krebber, and P.A. Silver. 1998. A member of the Ran-binding protein family, Yrb2p, is involved in nuclear protein export. *Proc. Natl. Acad. Sci. USA*. 95:7427–7432.

Traglia, H.M., J.P. O'Connor, K.S. Tung, S. Dallabrida, W.C. Shen, and A.K. Hopper. 1996. Nucleus-associated pools of Rna1p, the *Saccharomyces cerevisiae* Ran/TC4 GTPase activating protein involved in nucleus/cytosol transit. *Proc. Natl. Acad. Sci. USA*. 93:7667–7672.

Vallen, E.A., M.A. Hiller, T.Y. Scherson, and M.D. Rose. 1992. Separate domains of KAR1 mediate distinct functions in mitosis and nuclear fusion. *J.*

Cell Biol. 117:1277–1287.
Weis, K., I.W. Mattaj, and A.I. Lamond. 1995. Identification of hSRP1 α as a functional receptor for nuclear localization sequences. *Science*. 268:1049–1053.
Wente, S.R. 2000. Gatekeepers of the nucleus. *Science*. 288:1374–1377.
Wozniak, R.W., M.P. Rout, and J.D. Aitchison. 1998. Karyopherins and kissing cousins. *Trends Cell Biol*. 8:184–188.
Wu, J., M.J. Matunis, D. Kraemer, G. Blobel, and E. Coutavas. 1995. Nup358, a cytoplasmically exposed nucleoporin with peptide repeats, Ran-GTP binding sites, zinc fingers, a cyclophilin A homologous domain, and a leucine-rich region. *J. Biol. Chem*. 270:14209–14213.
Yano, R., M.L. Oakes, M.M. Tabb, and M. Nomura. 1994. Yeast Srp1p has homology to armadillo/plakoglobin/β-catenin and participates in apparently multiple nuclear functions including the maintenance of the nucleolar structure. *Proc. Natl. Acad. Sci. USA*. 91:6880–6884.
Yaseen, N.R., and G. Blobel. 1999a. GTP hydrolysis links initiation and termination of nuclear import on the nucleoporin Nup358. *J. Biol. Chem*. 274: 26493–26502.
Yaseen, N.R., and G. Blobel. 1999b. Two distinct classes of Ran-binding sites on the nucleoporin Nup 358. *Proc. Natl. Acad. Sci. USA*. 96:5516–5521.